ELSEVIER

Catalysis Today 28 (1996) 147–157

CATALYSIS TODAY

The promoting effect of noble metal addition on niobia-supported cobalt catalysts

F.B. Noronha [a,b], A. Frydman [a,c], D.A.G. Aranda [a], C. Perez [a], R.R. Soares [a], B. Morawek [b], D. Castner [c], C.T. Campbell [c], R. Frety [b], M. Schmal [a,*]

[a] *NUCAT / PEQ / COPPE-Escola Quimica, Univ. Federal Rio de Janeiro, Rio de Janeiro, Brazil*
[b] *Inst. Recherches Catalyse and LACE / CNRS, Villeurbanne, France*
[c] *Inst. Chemistry, University of Washington, Washington, DC, USA*

Abstract

The promoting effects of a noble metal (Pd, Pt, Rh) added to Co/Nb_2O_5 catalysts were studied by varying the Me/Co atomic ratios. Acid niobium was calcined to niobium pentoxide. The surface and bulk structures of the calcined materials were characterized by XPS and TPR techniques. The catalytic performance was obtained with CO hydrogenation. The addition of a noble metal promoted the reduction of Co^{3+} and Co^{2+} phases at the surface. XPS results revealed that Co^{2+} species are well dispersed as a thin layer around the niobium support together with Co_3O_4 crystallites islands. The Co_3O_4/Co^{2+} ratio depends on the surface area of the support. XPS measurements also revealed that PdO, Rh_2O_3 and PtO_2 are the main phases in the mono and bimetallic catalysts. The activity of the bimetallic catalysts increased and the stability was already attained. The selectivities towards C_5^+ and oxygenates increased with the addition of Rh up to an atomic ratio of 0.5 and decreased beyond that. This behavior is similar for both temperatures of reduction at 573 and 773 K.

Keywords: Niobia-supported cobalt catalysts; Noble metal addition

1. Introduction

Cobalt based catalysts have been frequently used in the Fischer–Tropsch synthesis. The nature of the support has a strong influence on the catalytic properties for the CO hydrogenation [1,2].

This reaction has also been studied on metal supported reducible oxides, like titanium and niobium oxides [3–7] and the main observation was that the product selectivity changed, depending on the reduction temperature and the metal loading. The niobia-supported catalysts showed a higher selectivity toward saturated hydrocarbons compared to the alumina supported ones, after reduction at high temperatures [5–7].

The important feature is that Nb_2O_5 in the presence of a metal presents a SMSI effect [8,9]. Silva et al. [5] showed that Co/Nb_2O_5 after reduction at 773 K presents a strong SMSI effect and that it is destroyed after oxidation in agreement with the literature [8,10]. In particu-

* Corresponding author.

SSDI 0920-5861(95)00218-9

lar for the CO hydrogenation, Haller and Resasco [10], as well as Kunimori et al. [3], have shown that the SMSI effect is destroyed during the reaction itself, due to the presence of water. However, Silva et al. [5] and Frydman et al. [6] found that the activity was not completely reversed and that the selectivity was drastically modified, enhancing the longer carbon chains after high temperature of reduction. These results demonstrate strong interaction of cobalt with the support and its rearrangement, suggesting that new species promoted the sites which increase the hydrocarbons toward longer chains.

Now, the question is what happens when a second metal is added to Co/Nb_2O_5 catalysts? Noronha et al. [11] showed that the addition of copper to Pd/Nb_2O_5 diminished the SMSI effect. The addition of a noble metal can also change the cobalt properties [12–14]. Lapidus et al. [12] reported data of the CO hydrogenation with Ru, Pd and Pt added to Co/Al_2O_3 catalysts and found that they are also more selective in C_5^+ hydrocarbons.

The main objective of this work is to determine the effect of the addition of a second metal to the Co/Nb_2O_5 catalysts and to understand better the surface properties of the metallic phases due to the interaction with the support by evaluating their performance in the CO hydrogenation reaction. Besides the reaction itself, the catalysts were characterized by XPS, TPR and DRS techniques.

2. Experimental

2.1. Preparation of the catalysts

Niobium pentoxide was obtained by calcination of niobium acid (CBMM) at two different temperatures: 873 K for 4 h, resulting in a crystalline form, T or TT, of niobium pentoxide (25 m^2/g) and 823 K for 2 h (50 m^2/g).

The catalysts were prepared by impregnation of cobalt, palladium and rhodium nitrates or platinum hexachloride on both supports, as described elsewhere [15–17]. The cobalt loading was 5% on Pd–Co and Pt– Co and different Me/Co atomic ratios. On the Rh–Co system the cobalt content was 2%, keeping atomic ratios of the same order as above. The following catalysts and their compositions are summarized in Table 1

2.2. Characterization

TPR experiments were performed in a conventional apparatus, as described elsewhere [11], using mixtures of 1.73% H_2/Ar and 2% O_2/He, respectively. In addition, DRS measurements were carried out in the oxide or passivated form in a Cary 5 UV–DRS system. XPS measurements were performed using monochromatic Al Kα radiation. The Nb 3d = 206.4 eV of the support was used as reference.

Table 1
Composition of the bimetallic catalysts

Pd wt.-%	Co wt.-%	Pd/Co ratio [a]	Pt wt.-%	Co wt.-%	Pt/Co ratio [a]	Rh wt.-%	Co wt.-%	Pd/Rh ratio [a]
1.3	–	–	0.5	–	–	0.9	–	–
2.1	2.0	0.53	0.5	5.0	0.03	0.3	2.0	0.09
1.6	5.0	0.17	–	5.0	–	0.6	1.9	0.19
–	5.0	–				0.7	1.8	0.24
						1.9	2.3	0.72
						–	1.9	–

[a] Atomic ratio.

2.3. Catalytic activity

The reaction was performed with Pt–Co and Rh–Co supported on Nb_2O_5 catalysts, after being treated at different reduction temperatures: 573 K (LTR) and 773 K (HTR). The following conditions were used in the microreactor, keeping conversions below 20%: reactant mixture of 4% $He/H_2/CO$ ($H_2/CO = 2$); total pressure 0.1 MPa, temperature 533 K and time on stream of approximately 30 h. Data were taken every hour in the first 8 h and after running 25–30 h. Selectivities were obtained at isoconversion after attaining steady state condition.

3. Results and discussion

3.1. Reducibility of the bimetallic catalysts

The formation of a bimetallic system and the transformations occurring during the reduction were studied, using different temperature programmed techniques, like TPR and TPO. The states of the intermediate oxide forms as isolated or bimetallic and alloy species were analyzed by complementary techniques to achieve a real understanding of the effect of a second metal supported on niobium oxide, known as a reducible oxide at elevated temperatures.

The TPR profiles are displayed in Fig. 1. The monometallic catalysts of all series have a behavior of reduction which is similar to those presented in the literature [5,11,18]. Palladium oxide is reduced at room temperature (RT) to

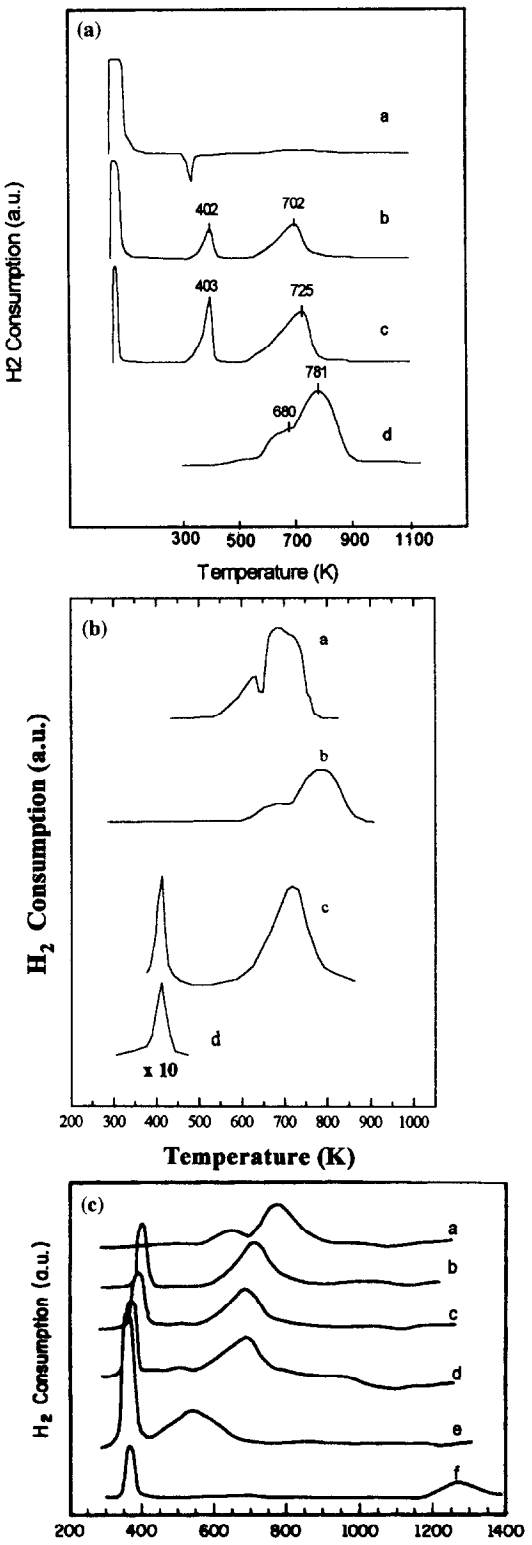

Fig. 1. (top) Reduction profiles of the Pd–Co niobia-supported catalysts. (a) Pd/Nb_2O_5; (b) $Pd_{35}Co_{65}/Nb_2O_5$; (c) $Pd_{15}Co_{85}/Nb_2O_5$; (d) $5\%Co/Nb_2O_5$.(middle) Reduction profiles of the Pt–Co niobia-supported catalysts. (a) Physical Mixture $Co_3O_4 + Nb_2O_5$; (b) $5\%Co/Nb_2O_5$; (c) Pt_3Co_{97}/Nb_2O_5; (d) Pt/Nb_7O_5. (bottom) Reduction profiles of the Rh–Co niobia-supported catalysts. (a) Co/Nb_2O_5; (b) $Rh_{09}Co_{91}/Nb_2O_5$; (c) $Rh_{19}Co_{81}/Nb_2O_5$; (d) $Rh_{24}Co_{76}/Nb_2O_5$; (e) $Rh_{72}Co_{28}/Nb_2O_5$; (f) Rh/Nb_2O_5.

metallic palladium and displays one desorption peak at 341 K, which is attributed to the desorption of reversible hydrogen from the palladium surface and to the decomposition of palladium hydride [19]. In addition, H_2 consumption is also observed at elevated temperatures (473 K), in general attributed to a partial reduction of the support [20].

Rhodium supported catalyst (Rh/Nb_2O_5) profile shows a sharp peak at 367 K, suggesting a single reduction step of Rh^{3+} to Rh^0, which is in good agreement with van't Blick on Rh/Al_2O_3 [18]. It means that, after calcination, rhodium oxide is in the Rh_2O_3 form. The Pt/Nb_2O_5 profile is similar, showing a well defined peak at 411 K, indicating that it has only one Pt structure in the calcined form. DRS results show indeed the presence of PtO_2 at the surface [15].

Noteworthy is the reduction of Co/Nb_2O_5 catalyst. For the 5% Co/Nb_2O_5 catalyst, there are two main peaks at 680 and 781 K (Fig. 1a). Recently, Frydman et al. [17] reported the presence of both Co_3O_4 particles and Co^{2+} species, probably linked to the support. Then, the H_2 consumption at 680 K could be attributed to the reduction of Co_3O_4 particles and the peak around 781 K due to the reduction of Co^{2+} species. The profile of a physical mixture of $Co_3O_4 + Nb_2O_5$ and DRS spectra confirms that Co_3 O_4 is the main phase in the cobalt catalyst [15].

The TPR profiles of the bimetallic catalysts display quite different behaviors from the monometallics. The shapes and temperatures of reduction are dependent on the second metal added to cobalt. The profiles are not only a single superposition of the monometallic profiles, showing different temperatures of reduction peaks. The H_2 consumptions varied as a function of the metal added to cobalt.

Profiles of the $Pd–Co/Nb_2O_5$ catalysts are shown in Fig. 1a for different Pd/Co ratios. They show typically three temperatures of reduction, namely at RT, 400 and around 700–725 K. These peaks are shifted to lower temperatures when compared to the Co/Nb_2O_5 catalyst. It seems that the addition of palladium promotes the reduction of Co_3O_4.

The $Pt–Co/Nb_2O_5$ and $Rh–Co/Nb_2O_5$ profiles are displayed in Fig. 1b and Fig. 1c, for different Me/Co atomic ratios together with the monometallic catalysts. The reduction occurs at two different temperature ranges. The first one around 400 K, corresponding to the simultaneous reduction of PtO_2 or Rh_2O_3 with $Co_3O_4 \rightarrow CoO$. The second at elevated temperatures, presented only one broad peak between 600 and 800 K corresponding to $Co^{2+} \rightarrow CoO$ reduction, shifted down 70 K when compared to the Co/Nb_2O_5 catalyst. The band at 728 nm related to Co^{3+} disappeared from DRS spectra [15]. Thus, Pt^0 promotes the reduction of Co_3O_4 after low temperature (510 K), as shown in Fig. 1b. These profiles also reveal a bimetallic formation and a strong influence of metallic Pt and Rh on the reduction of cobalt oxide.

For the Rh/Nb_2O_5 and Pt/Nb_2O_5 catalysts, the hydrogen consumptions correspond exactly to the theoretical values and, thus, indicating full reduction. It is more complex for the Co/Nb_2O_5 catalyst. In the 2% cobalt catalyst, we observed an excess of H_2 consumption of approximately 23% of H_2 above 623 K, due to the partial reduction of Nb_2O_5 in contact with the metal.

Now, analyzing the H_2 consumption on bimetallic catalysts we have the following observations:

For the $Pd–Co/Nb_2O_5$ catalysts, the H_2 consumption at RT is higher than the theoretical amount needed to reduce PdO to Pd^0. It is also higher in the region between 298–473 K where Co_3O_4 reduces to CoO. Therefore, it seems that Pd^0 promotes the reduction of Co_3O_4 particles at lower temperatures. Magnetic measurements confirm that 3% of cobalt at RT and 12% after reduction at 473 K are in the metallic form [16]. However, the promoting effect of Pd^0 decreases with higher cobalt loadings. Similar considera-

tions should be extended to the Pt–Co and Rh–Co catalyst for the temperature range between 340–430 K.

For Pd–Co, Pt–Co and Rh–Co catalysts, the amount of H_2 consumed in the high temperature range is higher than that necessary to reduce CoO and Co^{2+} to Co^0. Magnetic measurements showed that, after reduction at 873 K, only Co^0 is present. This was also verified by TPO for Pt–Co and Co/Nb_2O_5 catalysts [15]. Therefore, this excess of hydrogen consumption can be ascribed to a partial reduction of the support, as it was seen for Co/Nb_2O_5 catalyst. The behavior of the $Rh–Co/Nb_2O_5$ catalyst was somewhat surprising, because the H_2 consumption exceeded extremely the stoichiometric value for the reduction of the oxides to the metallic phase. This excess decreases as rhodium content increases and disappears with rhodium alone.

3.2. X-Ray photoelectron spectroscopy

Figs. 2 and 3 show the XPS lineshapes of Co 2p spectra for $Rh–Co/Nb_2O_5$, $Pd–Co/Nb_2O_5$ and $Pt–Co/Nb_2O_5$ calcined catalysts, respectively.

For the Pd/Nb_2O_5 and $Pd_{35}Co_{65}/Nb_2O_5$ catalysts, the binding energies for the Pd $3d_{5/2}$ peak were 337.0 and 336.9 eV, respectively

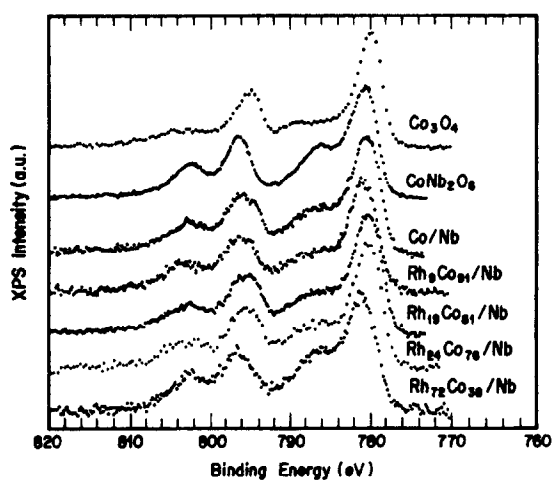

Fig. 2. XPS Co 2p spectra of the calcined $Rh–Co/Nb_2O_5$ catalysts.

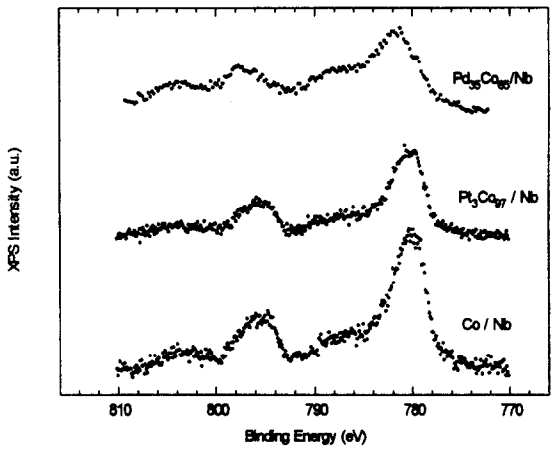

Fig. 3. XPS Co 2p spectra of the calcined $Pd–Co/Nb_2O_5$ and $Pt–Co/Nb_2O_5$ catalysts.

(Table 2). According to the literature, these values correspond to the presence of PdO [21]. On the other hand, on the Rh–Co and Pt–Co catalysts, two peaks were observed for the Rh $3d_{5/2}$ and Pt $4f_{7/2}$ suggesting a partial reduction of both Rh_2O_3 and PtO_2 by the X-ray beam.

In order to identify the cobalt species by XPS, the binding energy (BE) of Co $2p_{3/2}$ peak and spin-orbit splitting values of reference compounds are listed in Table 2. The BE values found for the two different cobalt oxides (CoO

Table 2
Binding energies of the main elements in the niobia-supported catalysts and reference compounds

Catalysts	Binding Energy (eV)				
	Pd $3d_{5/2}$	Rh $3d_{5/2}$	Pt $4f_{7/2}$	Co $2p_{3/2}$	ΔE
Pd	337.0	–	–	–	–
$Pd_{35}Co_{65}$	336.9	–	–	781.3	16.1
Rh	–	308.6 (310.2)	–	–	–
Rh_8Co_{92}	–	308.7 (310.2)	–	780.8	15.4
$Rh_{16}Co_{84}$	–	308.5 (310.3)	–	780.3	15.3
$Rh_{19}Co_{81}$	–	308.6 (310.2)	–	780.4	15.4
$Rh_{42}Co_{58}$	–	308.9 (310.1)	–	780.8	15.6
Pt	–	–		–	–
Pt_3Co_{97}	–	–	71.6 (75.1)	780.4	15.4
2% Co	–	–	–	780.5	15.4
5% Co	–	–	–	781.6	15.8
Co_3O_4	–	–	–	779.9	15.1
CoO	–	–	–	780.4	16.0
$CoNb_2O_6$	–	–	–	780.3	16.1

and Co_3O_4) are very similar and it does not allow a distinction between them. On the other hand, the secondary features (shake-up, spin-orbit splitting) of the spectra are different and can be used to distinguish them. On the Co_3O_4, the satellite is practically absent while CoO and $CoNb_2O_6$ show a strong satellite peak. Furthermore, the energy separation between the Co $2p_{3/2}$ peak and the Co $2p_{1/2}$ is close to 15.2 eV for Co_3O_4 but substantially larger for pure Co^{2+} oxides like CoO (15.9 eV), as shown in Table 2.

The Co 2p lineshapes of the Co/Nb_2O_5 catalysts suggest the presence of different Co species on the surface. The broadening of the Co $2p_{3/2}$ line and the spin-orbit splitting values indicates that the main cobalt species on both Co/Nb_2O_5 catalysts was Co_3O_4.

Several cobalt species have been detected in the precursors of supported cobalt catalysts [2,22,23]. The case of alumina-supported cobalt has been well described. At least, three different cobalt species have been identified: Co_3O_4 particles, Co^{2+} species and $CoAl_2O_4$, a surface compound with the spinel structure. In addition, the fraction of each phase can vary with cobalt loading. Thus, the amount of Co_3O_4 particles increases at higher cobalt loading [23]. Ho et al. [22] used XPS to characterize the state of cobalt in a series of Co/TiO_2 catalysts with different cobalt contents. They showed that the cobalt phase was primarily present as a highly dispersed surface cobalt species in the 0.5 and 1.0 wt.-% Co/TiO_2 samples. By increasing the amount of cobalt, discrete Co_3O_4 particles were formed, in addition to Co^{2+} species.

Therefore, our results are in good agreement with the model proposed in the literature. In such a model, a Co/Nb_2O_5 catalyst with a support having a low surface area would show a higher amount of Co_3O_4 particles. This can explain the similar fraction of Co_3O_4 particles on both Co/Nb_2O_5 catalysts with different cobalt loadings.

The Co 2p XPS spectra of the bimetallic catalysts also suggest the presence of different cobalt species (Fig. 2). In the case of Rh–Co/Nb_2O_5 catalysts, an experimental procedure, described elsewhere [17], was used to resolve the Co 2p lineshapes of the catalysts into contributions from Co_3O_4 and Co^{2+} features. The Co 2p spectrum of the catalysts was compared to a Co 2p spectrum of pure Co_3O_4. The difference between these two spectra was then compared to a Co 2p spectrum of pure $CoNb_2O_6$. It was clear that the difference spectrum was essentially identical to the $CoNb_2O_6$ reference spectrum meaning that in all catalysts, the Co 2p spectra were well fit by a simple superposition of Co_3O_4 and Co^{2+} (specially $CoNb_2O_6$) features. Since, the lineshapes of other Co^{2+} oxides like CoO are very similar to that of $CoNb_2O_6$, we could not definitively determine whether the Co^{2+} species detected on the supported catalysts is Co niobate or another Co^{2+} oxide.

From the experimental XPS intensity ratios for Co/Nb, Rh/Nb and Rh/Co, it was seen that Rh is surface-enriched relative to Co, since, the Rh/Co surface atomic ratios are larger than the bulk ratios by up to a factor of 2 [17]. Through XPS intensities, several model structures were postulated to represent the surface of the calcined bimetallic catalysts and to rule out others. The model that best described the experimental XPS intensities considered a Co^{2+} surface phase covering the surface of the Nb_2O_5 particles in the spaces between bilayer islands of Rh_2O_3 on top of Co_3O_4. The amount of Co in the Co^{2+} phase was very small, so that 78–90 wt.-% of the total Co was present in the Co_3O_4 phase.

On the Pd–Co/Nb_2O_5 catalyst, the XPS analysis also revealed the presence of Co_3O_4 particles and a Co^{2+} surface phase (Fig. 3) [16]. The Co 2p lineshape of the $Pd_{35}Co_{65}/Nb_2O_5$ bimetallic catalyst showed a Co $2p_{3/2}$ peak at 781.3 eV, a strong shake up satellite around 786 eV and a spin-orbit coupling of 16.1 eV suggesting that the fraction of the Co^{2+} surface phase was quite pronounced.

The TPR and XPS results allowed us to postulate a model which represents these

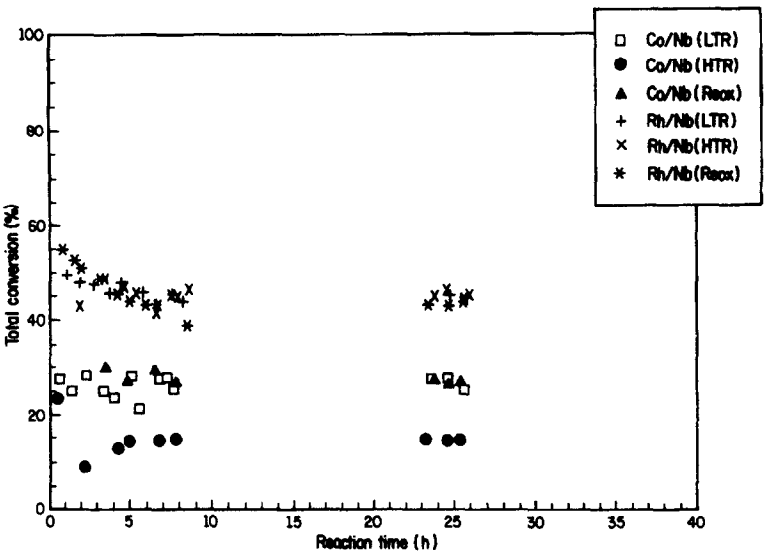

Fig. 4. Total conversion with time on stream

bimetallic catalysts. From the TPR profiles of the Pd–Co/Nb_2O_5 catalysts, it was seen that the presence of palladium promoted not only the reduction of Co_3O_4 particles but also the cobalt surface phase, represented by the second TPR peak. These results can be explained by the presence of the palladium oxide particles spread over the Co^{2+} layer or interfaced with Co_3O_4. The same model can be proposed for the Pt–Co catalysts, since, similar TPR and XPS results were obtained.

3.3. CO hydrogenation

Figs. 4 and 5 show the rate of CO conversion as a function of time for all Rh–CO and Pt–CO catalysts reduced at 573 and 773 k. The steady state was obtained very quickly for the bimetal-

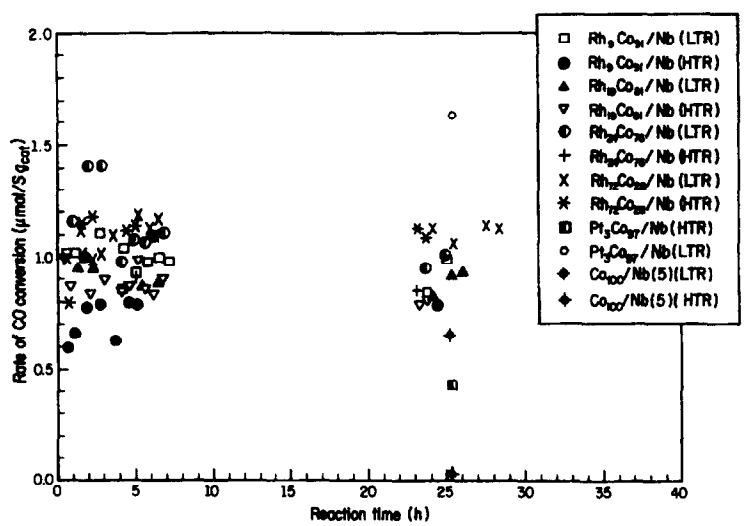

Fig. 5. Rate of CO conversion with time on stream

lic catalysts already after 8 h. The activity of Rh/Nb_2O_5 was 3 fold higher than for Co/Nb_2O_5 after LTR. The activities decreased with the increase of the temperature of reduction and increases with the addition of a second metal. No significant deactivation was observed on the bimetallic catalysts, only the initial activity of Rh/Nb_2O_5 catalyst decays drastically, but stabilizes after 8 h.

The effect of the temperature of reduction was significant for the monometallics. Comparing the activities after LTR and HTR the decay was 7 fold for Co/Nb_2O_5 while for Rh/Nb_2O_5 it was only 1.5. In order to verify the SMSI effect, we checked its reversibility by performing the reaction after HTR and then after a sequence of oxidation at 673 K and reduction at LTR. Results show, in accordance with former data [5,6], that the reversibility of the SMSI effect on the Co/Nb_2O_5 is only partially restored, however, it was completely reverted on Rh/Nb_2O_5, in agreement with Kunimori's observations [3].

The addition of Pt to Co/Nb_2O_5, as displayed in Fig. 5 increases the activity that decays drastically after HTR. This is expected because Pt favors the spillover of H_2 on the neighborhood of the metals [23], promoting the reduction of cobalt. Unfortunately, after HTR the active bimetallic species are not predominant.

On the contrary, the effect of the reduction temperature on the bimetallic catalyst Rh–Co was rather weak in the CO conversion. The reaction rate is approximately of the same order at LTR and HTR. We proposed from XPS data a model system assuming that rhodium is dispersed over Co_3O_4 islands and on dispersed Co^{2+} species covering the support. Therefore, after reduction the surface of the bimetallic system is not substantially modified, and these sites, even if some alteration occurs with respect to the initial state, are able to recover a permanent equilibrium state with time on stream.

Table 3
Product selectivity for the CO hydrogenation

Catalyst	$T_{reduction}$	Selectivity (%)					
		C_1	C_{2-4}	C_5^+	C_nOH	$C_2^=/C_2$	CO_2
Co	LTR [a]	52.3	29.3	16.1	–	11.4 [c]	2.3
	HTR [b]	14.1	34.8	48.8	–	17.1 [c]	2.3
$Rh_{09}-Co_{91}$	LTR	26.5	26.42	37.44	8.94	0.97	0.69
	HTR	17.5	14.08	62.26	5.65	1.03	0.86
$Rh_{19}-Co_{81}$	LTR	23.49	20.53	51.85	2.37	0.76	0.23
	HTR	15.09	12.43	67.1	4.05	1.26	0.34
$Rh_{24}-Co_{76}$	LTR	22.99	19.03	53.92	3.96	1.47	0.19
	HTR	14.89	11.74	68.64	3.37	2.19	1.36
$Rh_{72}-Co_{28}$	LTR	20.15	13.17	63.05	1.91	1.53	1.72
	HTR	11.86	9.34	71.28	1.67	4.31	5.85
Rh	LTR	27.89	22.62	38.58	4.78	1.56	6.13
	HTR	26.46	24.01	35.38	4.74	2.12	9.41
$Pt_{03}-Co_{97}$	LTR	55	5	32	–	–	8
	HTR	20	7	38	–	–	35

[a] LTR: low temperature reduction = 573 K.
[b] HTR: high temperature reduction = 773 K.
[c] $C_2^=/C_2$: ethene/ethane ratio.

3.4. Product selectivity

The product selectivity obtained at isoconversion varied with the addition of a second metal and with the reduction temperature, as presented in Table 3. In Table 3 are given the oxygenated products, namely ethanol, isopropanol, propanol and butanol together with the selectivities of C_{2-4}, $C_2^=/C_2$ ratio and CO_2.

Noteworthy are the behaviors of the CH_4 and C_5^+ selectivities with the reduction temperature and the rhodium content added to cobalt. While at LTR the selectivity of C_1 on Co/Nb_2O_5 is high and C_5^+ is low, this situation is reversed after HTR. These results show strong interaction of cobalt with the support and its rearrangement, suggesting that new species promoted the sites which increase the hydrocarbons towards longer chains [6,12].

Results reported in [5] have shown that the selectivity changes with time on stream. The selectivity towards C_5^+ increases significantly during the first 8 h on stream before stabilizing for more than 50 h. Therefore, the reaction modifies the nature of the sites during the activation with time on stream. Lee and Bartholomew [24] proposed mechanisms involv-

ing the formation of an intermediate (CH_xO) or formiate methoxy species, on different sites of the metal, in the presence of the support, due to the spillover of H_2 and CO over the support. This model is consistent for catalysts with low cobalt loading which contains a large fraction of aluminates or Co^{2+} species dispersed over the support and which are unable to dissociate CO and H_2.

Nevertheless, the selectivity on Rh/Nb_2O_5 is different, presenting large molecules of olefins and alcohols. Iizuka et al. [25] reported the formation of such products on a Rh/Al_2O_3 catalyst.

For bimetallic catalysts, by increasing the Rh content, C_1 and C_5^+ selectivities attained minimum and maximum values, respectively, at a Co/(Rh + Co) ratio of about 0.5. Methane was low while C_5^+ was enhanced by a factor 6–7, together with formation of oxygenates due to the presence of rhodium. The C_5^+ products increase markedly with the increase of Rh, attaining a maximum selectivity of ca. 70% and decrease with higher contents, as shown in Fig. 6. The same behavior is seen for $C_2^=/C_2$ ratio and CO_2 selectivities after HTR. These results are in good agreement with Iglesia et al. [26] on $Ru–Co/Al_2O_3$ catalyst. They obtained, at similar conditions, 85% of C_5^+ products, rather close to our results. With respect to the formation of alcohols, it attains a maximum with the addition of small amounts of Rh in the bimetallic catalyst but decreases to a minimum around the ratio 0.5. This shows synergetic effects of Rh in the presence of Co. In the present case, the selectivity changed drastically. On the contrary, van't Blik [19] did not observe marked changes on selectivity for Rh–Co supported on Al_2O_3 and TiO_2 in the CO/H_2 reaction at 523 K.

Lee et al. [27] suggested that rhodium in the ionic state (Rh^{n+}) favors the formation of methanol while Rh^0 favors the formation of ethanol. However, they demonstrated that Co–Rh particles after reduction were enriched with Co and that rhodium initially present as Rh^0 is oxidized due to CO adsorption. The Rh–Rh

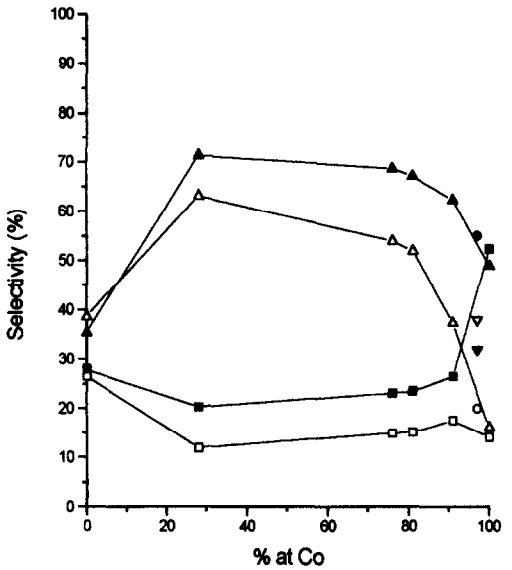

Fig. 6. Product selectivities of C_5^+ and C_1 as a function of cobalt atomic ratio. (△) Rh–Co: C_5^+ after LTR; (▲) Rh–Co: C_5^+ after HTR; (■) Rh–Co: C_1 after LTR; (□) Rh–Co: C_1 after HTR; (▼) Pt–Co: C_5^+ after LTR; (▽) Pt–Co: C_5^+ after HTR; (●) Pt–Co: C_1 after LTR; (○) Pt–Co: C_1 after HTR.

bond breaks, forming carbonyls ($Rh(CO)_2$), in which Rh is in the ionic state Rh^{1+}. Our results are consistent with the conclusion of Lee et al. Therefore, with increasing Rh^0 at the surface, during CO adsorption it provides Rh^{1+}, favoring the formation of oxygenated compounds. Nevertheless, the CO on platinum particles is basically adsorbed in the linear form [13], which explains the lower selectivity towards the oxygenated products in $Pt–Co/Nb_2O_5$.

We try to explain this selectivity behavior on the basis of our TPR and XPS results discussed above. The surface model presented by Frydman et al. [17] suggests schematically the presence of Co^{2+} species covering practically the whole niobium oxide surface as a thin and well dispersed layer, together with isolated islands of Co_3O_4 crystals covered with rhodium particles. As shown in Fig. 6, the selectivity is a function of Rh added to Co and present similar shapes after LTR and HTR. The TPR results suggest an easy reduction of the supported phase, together with a small fraction of the support. After LTR, an important amount is consumed at lower tem-

peratures on the bimetallic catalysts whereas on Co/Nb_2O_5 alone it is rather limited. Moreover, the selectivity towards C_5^+ increases significantly. Therefore, these results provided us an insight to improve our model and to predict that Rh^0 is well dispersed over the Co^{2+} surface layer covering the support, being less dependent or the reduction temperature. Thus, the Co^{2+} species play a preferential role over niobium surfaces which corroborates with the proposed model of Lee et al. [27]. The presence of Rh^0 (Me^0) helps to reduce these Co^{2+} species and Co_3O_4 particles at LTR and HTR. Therefore, during the reaction the reduced particles can easily be transformed to Rh^{n+} and Co^{n+} in the bimetallic catalysts, which are potential sites for the methylene insertion, as well as the CO insertion to account for oxygenates and C_5^+ products. However, at higher content of rhodium, larger particles may occur decreasing the efficiency of formation of these ionic species due to a better organization of both Rh and Co particles in the bimetallic system.

4. Conclusions

(1) The addition of a noble metal to the Co/Nb_2O_5 catalyst promoted pronounced changes in the reduction of cobalt. It helps to reduce the Co^{2+} and mainly the Co^{3+} species of Co_3O_4.

(2) XPS results made possible to confirm that the Co^{2+} species are well dispersed on a thin layer around the niobium oxide together with isolated Co_3O_4 crystallites. The Co_3O_4/Co^{2+} ratio depends on the surface area of the support. It has been shown that the noble metals are well dispersed over the Co_3O_4 and Co^{2+} species. In summary, Co_3O_4, Co^{2+} as well as PdO, Rh_2O_3 and PtO_2 are the main phases identified.

(3) The CO hydrogenation performed at two different reduction temperatures showed good stability for bimetallic catalysts, held constant up to 50 h with time on stream.

(4) The CO hydrogenation showed that the addition of Rh to Co/Nb_2O_5 in different amounts increased the C_5^+ hydrocarbons and the formation of oxygenated compounds after 573 and 773 K. However, they attained maximum yields around an atomic ratio of 0.5.

(5) On the basis of XPS, TPR and CO hydrogenation data, we have a good proposal for a model system. The Co^{2+} species are well dispersed as a thin layer at the surface and the noble metal is also well dispersed over the Co^{2+} species and Co_3O_4 islands, promoting their reduction. Therefore, during the reaction, CO promotes the ionic state of Me^{n+} and Co^{n+} forming sites for the insertion of methylene and CO to account for the growth of carbon chains and oxygenates. However, with increasing loading of noble metal it induces agglomeration of the particles, blocking the ionic sites.

Acknowledgements

We acknowledge CNPq, Pronac and Finep for the financial support of this work.

References

[1] R.C. Reuel and C.H. Bartholomew, J. Catal., 85 (1984) 63.
[2] D.G. Castner and D.S. Santilli, ACS Symp. Ser., 248 (1984) 39.
[3] K. Kunimori, H. Abe, E. Yamaguchi, S. Matsui and T. Uchijima, VIII Int. Cong. Catal., Berlin, 1984, Vol. 5, Verlag Chemie, Weinheim, 1984, p. 251.
[4] M.A. Vannice, J. Catal., 50 (1977) 228.
[5] R.R.C.M. Silva, M. Schmal, R. Frety and J.A. Dalmon, J. Chem. Soc., Faraday Trans., 89(21) (1993) 3975.
[6] A. Frydman, R.R. Soares and M. Schmal, Stud. Surf. Sci. Catal., C (1993) 2797.
[7] R.R. Soares, A. Frydman and M. Schmal, Catal. Today, 16 (1993) 361.
[8] S.J. Tauster, S.C. Fung and R.L. Garten, J. Catal., 55 (1978) 29.
[9] S.J. Tauster and S.C. Fung, J. Catal., 55 (1978) 29.
[10] G.L. Haller and D.E. Resasco, Adv. Catal., 36 (1989) 173.
[11] F.B. Noronha, M. Schmal, M. Primet and R. Frety, Appl. Catal., 78 (1991) 125.
[12] A.L. Lapidus, A.Y. Krylova, J. Rathousky, A. Zukal and M. Jancálková, Appl. Catal., 80 (1992) 1.
[13] E. Iglesia, S.C. Reys, S.L. Soled and R.J. Madon, Adv. Catal. Related Subjects, 39 (1993) 221.

[14] A. Fukuoka, F.S. Xiao, M. Ichikawa, D.F. Shriver and W. Hendeson, Shokubai, 32 (1990) 368.
[15] R.R. Soares, D.A.G. Aranda, A.J. Almeida and M. Schmal, XIV Cong. Ibero-Americano Catal., 1 (1994) 189.
[16] F.B. Noronha, P. Delichere, G. Bergeret, B. Moraweck, R. Frety and M. Schmal, to be published.
[17] A. Frydman, D.G. Castner, M. Schmal and C.T. Campbell, J. Catal., 152 (1995) 164.
[18] H.J.F. van't Blik, DSc.-Thesis, University of Technology, Eindhoven, 1984.
[19] T.C. Chang, J.J. Chen and C.T. Yeh, J. Catal., 96 (1985) 51.
[20] Z. Hu, K. Kunimori and T. Uchijima, Appl. Catal., 69 (1991) 253.
[21] L. Otto, L.P. Haack and J.E. de Vries, Appl. Catal. B, 1 (1991) 1.
[22] S.W. Ho, M. Houalla and D.M. Hercules, J. Phys. Chem., 94 (1990) 6396.
[23] R.L. Chin and D.M. Hercules, J. Chem., 86 (1982) 360.
[24] W.H. Lee and C.H. Bartholomew, Spring Meet. California Catal. Soc., 1986.
[25] T. Iizuka, Y. Tanaka and K.J. Tanabe, J. Mol. Catal., 17 (1982) 381.
[26] E. Iglesia, S.L. Soled, A. Fiato and G.H. Via, J. Catal., 143 (1993) 345.
[27] G.V. Lee, B. Schuller, H. Post, T.L.F. Favre and V. Ponec, J. Catal., 98 (1986) 522.